

# Human Relaxin-2 Fusion Protein Treatment Prevents and Reverses Isoproterenol-Induced Hypertrophy and Fibrosis in Mouse Heart

Junhui Sun, PhD;\* Weidong Hao, PhD;\* Natasha Fillmore, PhD; Hanley Ma, BA; Danielle Springer, VDM; Zu-Xi Yu, MD, PhD; Agnieszka Sadowska, MS; Andrew Garcia, BA; Ruoyan Chen, BS; Vanessa Muniz-Medina, BS; Kim Rosenthal, MS; Jia Lin, MS; Denison Kuruvilla, PhD; Jane Osbourn, PhD, OBE; Sotirios K. Karathanasis, PhD; Jill Walker, PhD; Elizabeth Murphy, PhD

**Background**—Heart failure is one of the leading causes of death in Western countries, and there is a need for new therapeutic approaches. Relaxin-2 is a peptide hormone that mediates pleiotropic cardiovascular effects, including antifibrotic, angiogenic, vasodilatory, antiapoptotic, and anti-inflammatory effects in vitro and in vivo.

**Methods and Results**—We developed RELAX10, a fusion protein composed of human relaxin-2 hormone and the Fc of a human antibody, to test the hypothesis that extended exposure of the relaxin-2 peptide could reduce cardiac hypertrophy and fibrosis. RELAX10 demonstrated the same specificity and similar in vitro activity as the relaxin-2 peptide. The terminal half-life of RELAX10 was 7 days in mouse and 3.75 days in rat after subcutaneous administration. We evaluated whether treatment with RELAX10 could prevent and reverse isoproterenol-induced cardiac hypertrophy and fibrosis in mice. Isoproterenol administration in mice resulted in increased cardiac hypertrophy and fibrosis compared with vehicle. Coadministration with RELAX10 significantly attenuated the cardiac hypertrophy and fibrosis compared with untreated animals. Isoproterenol administration significantly increased transforming growth factor  $\beta$ 1 (TGF- $\beta$ 1)-induced fibrotic signaling, which was attenuated by RELAX10. We found that RELAX10 also significantly increased protein kinase B/endothelial NO synthase signaling and protein S-nitrosylation. In the reversal study, RELAX10-treated animals showed significantly reduced cardiac hypertrophy and collagen levels.

**Conclusions**—These findings support a potential role for RELAX10 in the treatment of heart failure. (*J Am Heart Assoc.* 2019;8:e013465. DOI: 10.1161/JAHA.119.013465.)

**Key Words:** fibrosis • hypertrophy • NO

Cardiac injury leads to the development of hypertrophy and fibrosis, which typically transitions to heart failure (HF). HF is a cardiovascular disease affecting 26 million people worldwide in which the heart is unable to provide sufficient blood supply to the body, with 5- and 10-year mortality rates of 50% and 90%, respectively.<sup>1–3</sup> Current treatment strategies for HF include vasodilators, which

improve oxygenation, and diuretics, which relieve cardiac workload, as well as  $\beta$ -adrenergic and angiotensin signaling modulators that interfere with cardiac compression. These therapies have provided benefit to segments of the patient populations with HF, but not all patients show improvement and there is a need for new therapies that can reverse cardiac fibrosis and hypertrophy.

From the Cardiac Physiology Section/Cardiovascular Branch (J.S., N.F., H.M., E.M.), Murine Phenotyping Core (D.S.), and Pathology Core (Z.-X.Y.), National Heart, Lung, and Blood Institute/National Institutes of Health, Bethesda, MD; AstraZeneca, Gaithersburg, MD (W.H., A.S., A.G., R.C., V.M.M., K.R., J.L., D.K., S.K.K., J.W.); and AstraZeneca Ltd, Cambridge, United Kingdom (J.O.).

\*Dr Sun and Dr Hao contributed equally to this work.

Jane Osbourn is currently located at the Mogrify Ltd, 25 Cambridge Science Park, Cambridge, United Kingdom.

Sotirios K. Karathanasis is currently located at the Lipoprotein Metabolism Laboratory, National Heart, Lung, and Blood Institute, National Institutes of Health, Bethesda, MD; and NeoProgen, 323 W Camden St, Ste 600, Baltimore, MD 21201.

Jill Walker is currently located at the Horizon Therapeutics, 2000 Sierra Point Pkwy, Ste 400, Brisbane, CA 94005.

**Correspondence to:** Elizabeth Murphy, PhD, National Heart, Lung, and Blood Institute, National Institutes of Health, 10 Center Dr, Bldg 10, Room 6N248B, Bethesda, MD 20892. E-mail: murphy1@mail.nih.gov and Weidong Hao, PhD, AstraZeneca, One MedImmune Way, Gaithersburg, MD 20878. E-mail: weidong.hao@astrazeneca.com

Received May 30, 2019; accepted November 5, 2019.

© 2019 The Authors and AstraZeneca. Published on behalf of the American Heart Association, Inc., by Wiley. This is an open access article under the terms of the Creative Commons Attribution-NonCommercial License, which permits use, distribution and reproduction in any medium, provided the original work is properly cited and is not used for commercial purposes.

## Clinical Perspective

### What Is New?

- RELAX10 is a newly developed fusion protein of human relaxin-2 and the Fc of human antibody IgG1.
- RELAX10 was able to reverse isoproterenol-induced cardiac hypertrophy and fibrosis in mice.
- RELAX10 has an extended half-life to enable longer durations of the peptide exposure.

### What Are the Clinical Implications?

- RELAX10 may provide a novel treatment for heart failure.

The peptide hormone relaxin-2, originally identified as an important hormone during pregnancy, signals through the relaxin/insulin-like family peptide receptor 1 (RXFP1), a G-protein-coupled receptor that is expressed in reproductive tissues, bone, muscle, blood vessels, and various organs, including the heart.<sup>4–6</sup> Relaxin-2 signaling cascades have been well characterized and demonstrated the peptide mediates antifibrotic, angiogenic, vasodilatory, antiapoptotic, and anti-inflammatory effects. It has been shown in various tissues and in vivo models that relaxin-2 inhibits collagen biosynthesis and induces antifibrosis protective effects; thus, relaxin-2 has been emerging as a novel antifibrotic therapy.<sup>4,5,7–9</sup> A recombinant relaxin-2 peptide, called Serelaxin, has been pursued as a potential therapy for acute decompensated HF.<sup>10,11</sup> In clinical trials, intravenous (IV) administration of Serelaxin for 48 hours improved markers of cardiac, renal, and hepatic damage and reduced congestion.<sup>11,12</sup> However, these effects diminished rapidly on treatment termination. We hypothesized that the transient treatment benefits could be caused by the limited treatment duration and short half-life of Serelaxin because continuous infusion of Selaxin-2 peptide using subcutaneous implanted minipump has resulted in long-term benefits in animal studies.<sup>13–16</sup> This suggests that extended exposure to relaxin-2 could improve cardiac function. We have developed RELAX10 (a fusion protein composed of human relaxin-2 hormone and the Fc of a human antibody IgG1) with extended half-life to enable longer durations of the peptide exposure through subcutaneous (SC) dosing. Herein, we report the preclinical characterization of RELAX10, including in vitro activity and specificity, as well as the in vivo activity and pharmacokinetic profiles in rodents.

## Materials and Methods

The data that support the findings of this study are available from the corresponding author on reasonable request.

## Cloning and Expression of RELAX10

The RELAX10 gene sequences were synthesized by GeneArt (Regensburg, Germany) and supplied as plasmid DNA. The gene sequences were removed from GeneArt plasmid by restriction enzyme digestion with *Xba*I and *Not*I and cloned into the pHOE vector (AstraZeneca, Gaithersburg, MD) using the same restriction sites, leading to pHOE-RELAX10 plasmid. Plasmid was purified using PowerPrep maxi kit (Origene, Rockville, MD) and then transfected into CHO G22 cells using polyethylenimine. RELAX10 was purified from the CHO G22 supernatant using protein G HiTrap column (GE Healthcare, Pittsburgh, PA), and a size-exclusion column was used to remove any aggregates. The predicted mass for RELAX10 monomer is 34 718 Daltons (Da), and mass spectrum analysis showed a mass of 34 717 Da (see patent<sup>17</sup>).

## In Vitro cAMP Assay

The HitHunter cAMP assay (DiscoverX, Fremont, CA) was used to measure the cAMP produced after the relaxin-2 receptor-expressing cells (CHO-K1 RXFP1 Gs; DiscoverX) were stimulated with RELAX10. Recombinant human relaxin-2 (R&D Systems, Minneapolis, MN) was used as a positive control. The assay was performed on the basis of the manufacturer's protocol. The assay plate was read on a standard luminescence plate reader (EnVision; PerkinElmer, Shelton, CT) at 0.1 to 1 second/well. Data analysis was performed using statistical analysis software (GraphPad Prism, V6). To check the binding and activation specificity of RELAX10 for the RXFP1 receptor, the following cell lines were purchased from DiscoverX: (1) cAMP Hunter CHO-K1 RXFP2 Gs; (2) cAMP Hunter CHO-K1 RXFP3 Gi; (3) cAMP Hunter CHO-K1 RXFP4 Gi; and (4) cAMP Hunter CHO-K1 ADCYAP1R1 Gs/Gq. INSL3 (R&D Systems), INSL5 (Origene), Relaxin-3 (Origene), and PACAP1-27 (R&D Systems) were used as positive controls.

cAMP assays were performed as described for the RXFP1 cell line, except for cell lines RXFP3 and RXFP4, in which 25 or 20  $\mu$ mol/L forskolin (R&D Systems), respectively, was added to the dilution plate and serum-free medium to increase intracellular levels of cAMP as the ligands used in the assay will inhibit cAMP production. Experiments were performed at least twice.

## Vascular Endothelial Growth Factor Expression in THP-1 Cells

The ability of RELAX10 to induce the expression of vascular endothelial growth factor (VEGF) RNA, a known downstream target of relaxin-2,<sup>6</sup> was measured in THP-1 cells (ATCC, Manassas, VA) by quantitative real-time polymerase chain reaction. A total of  $10^6$  cells/mL was seeded in a 24-well flat-

bottom plate (Corning, Manassas, VA) in 400  $\mu$ L test media (RPMI-1640 without phenol red supplemented with 0.5% fetal bovine serum; Gibco, Fort Worth, TX), 1% penicillin/streptomycin (Gibco), and 0.05 mmol/L of  $\beta$ -mercaptoethanol (Gibco). After 24 hours of incubation at 37°C in the presence of 5% CO<sub>2</sub>, human relaxin-2 (R&D Systems) or RELAX10 was added to the cells in the plate for 2.5 hours at 37°C. RNA isolation and purification from THP-1 cells was performed using Qiagen's QiaShredder (Qiagen, Gaithersburg, MD) and RNA Plus Mini Kit (Qiagen), following the manufacturer's protocol. The mRNA concentrations were measured by NanoDrop (ThermoFisher Scientific, Waltham, MA), and samples were normalized to the same starting concentration. Reverse transcription–polymerase chain reaction samples were prepared using Express One-Step Superscript qRT-PCR kit (Invitrogen, Madison, WI), and primer/probe sets were as follows: VEGF-A human (ThermoFisher Scientific) and GAPDH human (ThermoFisher Scientific). Reverse transcription–polymerase chain reactions were performed using 7900HT Fast Real-Time PCR (Invitrogen) machine with cycle set up of: 1 cycle of 50°C for 15 minutes, 1 cycle at 95°C for 20 seconds, and 40 cycles at 95°C for 1 second, followed by 60°C for 20 seconds. The relative fold change in VEGF mRNA level was calculated by the comparative Ct (threshold cycle) method using GAPDH expression for normalization. Results were calculated as fold changes over no treatment control. Experiments were performed in triplicates, with an  $n > 2$ . Data were analyzed by paired 2-tailed  $t$  test using Prism GraphPad, V6.

### Pharmacokinetic Profiles of RELAX10

The pharmacokinetic profiles of RELAX10 were tested in both rat (8-week-old Wistar rats; Charles River, Wilmington, MA) and mouse (6–8 weeks old; C57BL/6J; The Jackson Laboratory, Bar Harbor, ME). The fusion protein RELAX10 was administered to the animals by the IV or SC route at dose ranging from 1 to 30 mg/kg. Blood samples were collected at various time points after drug administration. Samples were collected into a tube containing EDTA and placed on ice immediately. Samples were centrifuged for 15 minutes at 1000g within 30 minutes of collection. Aliquoted samples were stored at  $\leq -20^\circ\text{C}$  and later tested by ELISA to determine the protein concentration. The anti-Fc monoclonal antibody TM446 (AstraZeneca) was used to coat the ELISA plate. The horseradish peroxidase–conjugated polyclonal antibody from the Relaxin-2 detection ELISA kit (R&D Systems) was used as the ELISA detection reagent.

### Pharmacokinetic Analysis

Pharmacokinetic analysis was performed using noncompartmental analysis using Phoenix WinNonlin version 7.0 (Certara,

Princeton, NJ) software. The RELAX10 dose used for the in vivo prevention study was determined by pharmacokinetic simulation.

### Animals and Agent Administration via Micro-Osmotic Alzet Minipump

All animals were treated and cared for in accordance with the *Guide for the Care and Use of Laboratory Animals* (National Institutes of Health, revised 2011), and protocols were approved by the Institutional Animal Care and Use Committee of the National Heart, Lung, and Blood Institute. Male C57BL/6J mice were obtained from Jackson Laboratories at 11 weeks of age. For this initial study, we used only male mice to determine if Fc-relaxin provided protection. Future studies will examine sex differences. After 1 week of equilibration housing, micro-osmotic Alzet minipumps (model 1002; DURECT Corporation, Cupertino, CA) were implanted subcutaneously into mice. Mice are anesthetized using 1% to 3% isoflurane given by inhalation through a vaporizer. Each pump delivered a constant dose (0.25  $\mu$ L/h) of infused drug or vehicle.

### Prevention and Treatment Protocols Against Isoproterenol-Induced Hypertrophy

An initial pilot study was performed to establish the isoproterenol-mediated hypertrophy model delivered by micro-osmotic Alzet minipump and to confirm a reduction in hypertrophy with an angiotensin-converting enzyme inhibitor, enalapril. Mice were SC implanted with mini-osmotic pumps (Alzet model 1002) for continuous infusion of isoproterenol in PBS containing 0.002% ascorbic acid at 15 mg/kg per day for 2 weeks. Control mice were implanted with minipumps that delivered vehicle (PBS with 0.002% ascorbic acid) only.<sup>18–20</sup>

Six groups ( $n=8$  in each group) were designed for RELAX10 prevention study (protocol I): (1) vehicle control, minipump was infused with PBS containing 0.002% Na-ascorbate; (2) RELAX10 control, minipump was infused with PBS containing 0.002% Na-ascorbate; at day 0 and 7, mice were SC injected with 30 mg/kg (corresponds to 450 nmol/kg per day molecular weight of RELAX10=66,548.5) of RELAX10 diluted with PBS in 150  $\mu$ L total; (3) isoproterenol, minipump was infused with isoproterenol (15 mg/kg per day) in PBS with 0.002% Na-ascorbate; (4) isoproterenol+enalapril (Sigma-Aldrich, St Louis, MO), minipump was infused with isoproterenol (15 mg/kg per day) and enalapril (Sigma E6888; 2.5 mg/kg per day) in PBS with 0.002% Na-ascorbate PBS; (5) isoproterenol+relaxin-2, minipump was infused with isoproterenol (15 mg/kg per day) and relaxin-2 (0.5 mg/kg per day; 83 nmol/kg per day) in PBS with 0.002% Na-ascorbate PBS; (6) isoproterenol+RELAX10, minipump was infused with isoproterenol (15 mg/kg per day); at days 0 and 7, mice

were SC injected with 30 mg/kg of RELAX10 diluted with PBS in 150  $\mu$ L total. After 14 days, echocardiography was performed. After echocardiography, mice were euthanized and heart weight (HW), body weight (BW), and tibial length (TL) were measured.

Six groups (n=8 in each group) were designed for RELAX10 treatment study (protocol II): (1) vehicle control 10+14, minipump was infused with PBS containing 0.002% Na-ascorbate; at day 10, minipump was removed; and mice were euthanized at day 24; (2) isoproterenol 10+14, minipump was infused with isoproterenol (15 mg/kg per day) in PBS with 0.002% Na-ascorbate; at day 10, minipump was removed; and mice were euthanized at day 24; (3) isoproterenol 10+14 RELAX10, minipump was infused with isoproterenol (15 mg/kg per day) in PBS with 0.002% Na-ascorbate; at day 10, minipump was removed; at days 10 and 17, mice were SC injected with 30 mg/kg of RELAX10 diluted with PBS in 150  $\mu$ L total; and mice were euthanized at day 24; (4) isoproterenol 10+14 relaxin-2, minipump was infused with isoproterenol (15 mg/kg per day) in PBS with 0.002% Na-ascorbate; at day 10, minipump was removed and replaced with a new minipump infused with relaxin-2 (0.5 mg/kg per day); and mice were euthanized at day 24; (5) isoproterenol 10+14 enalapril, minipump was infused with isoproterenol (15 mg/kg per day) in PBS with 0.002% Na-ascorbate; at day 10, minipump was removed and replaced with a new minipump infused with enalapril (2.5 mg/kg per day); and mice were euthanized at day 24; (6) isoproterenol 10+14 enalapril and RELAX10, minipump was infused with isoproterenol (15 mg/kg per day) in PBS with 0.002% Na-ascorbate; at day 10, minipump was removed and replaced with a new minipump infused with enalapril (2.5 mg/kg per day); at days 10 and 17, mice were SC injected with 30 mg/kg of RELAX10 diluted with PBS in 150  $\mu$ L total; and mice were euthanized at day 24. After 24 days, mice were euthanized and HW, BW, and TL were measured. The treatment study was blinded. The treatment drugs were coded (A, B, C, etc).

Heart samples were also taken for measurement of fibrosis and collagen, and the investigator (JS and ZY) was blinded to the treatment. Each mouse heart was transversely divided into 3 portions: the apical portion for measuring collagen content, the midzone fixed first in 10% formalin and then 100% ethanol for histological analysis, and the basal portion for heart homogenate. Unfixed tissue was immediately snap frozen and stored in liquid nitrogen. Same portion from each animal was used for each individual assay to ensure standardization and enable intergroup comparisons.

### Preparation of Mouse Heart Tissue Homogenate

Heart homogenate of each basal portion of mouse heart was prepared in the dark to prevent S-nitrosylation decomposition.

The homogenate buffer contains (in mmol/L; all reagents are from Sigma-Aldrich): 300 sucrose, 250 HEPES-NaOH (pH 7.8), 1 EDTA, and 0.1 neocuproine (a copper chelating agent). An EDTA-free protease and phosphatase inhibitor tablet (Roche Diagnostics Corporation, Indianapolis, IN) was added to the homogenate buffer just before use. The snap-frozen heart tissue was transferred into Precellys (Bertin Technologies, Montigny-le-Bretonneux, France) homogenizing lysing kit beads CKmix tube. Homogenization was performed in a Precellys homogenizer (Bertin Technologies) chilled with liquid nitrogen. The samples were shaken twice at 6000 rpm for 20 seconds for each cycle, with 20-second interval. The homogenate was collected in dark amber tubes after quick spin at 2000g for 2 minutes at 4°C. Protein concentration of total heart homogenate was determined using the Bradford protein assay. Each heart homogenate was aliquoted in amber tubes, snap frozen in liquid nitrogen, and stored at  $-80^{\circ}\text{C}$ .

### Identification of Protein S-Nitrosylation With Modified CyDye-Maleimide Switch Method

A modified biotin switch method using sulfhydryl-mono-reactive CyDye-maleimide fluors (ThermoFisher Scientific) was applied to identify S-nitrosylation proteins.<sup>21–23</sup> Mouse heart homogenate (200  $\mu$ g) was blocked in HEN buffer (pH 8.0 in mmol/L: 250 HEPES-NaOH, 1 EDTA, and 0.1 Neocuproine) containing 20 mmol/L N-ethylmaleimide and 2.5% (w/v) SDS at 50°C for 20 minutes with frequent vortex. The N-ethylmaleimide was then removed by cold acetone precipitation at  $-20^{\circ}\text{C}$  for 20 minutes. After acetone removal, the protein pellets were resuspended in HEN buffer containing 1% (w/v) SDS and labeled with 5 mmol/L of Cy3-maleimide or Cy5-maleimide in the presence of 1 mmol/L of Na-ascorbate. After incubation on a rotating device for 3 hours at room temperature in the dark, equal amount of Cy3-maleimide- and Cy5-maleimide-labeled S-nitrosylation proteins from 2 samples were combined and subjected to nonreducing 4% to 12% Bis-Tris SDS-PAGE (ThermoFisher Scientific) in the dark. Equal amounts of GSNO (S-nitrosoglutathione)-treated BSA labeled with each Cy3-maleimide or Cy5-maleimide dye were also included to standardize fluorescence scanning using a Li-Cor Odyssey scanner (Li-Cor Biosciences, Lincoln, NE) at 700 and 800 nm for Cy3 and Cy5 S-nitrosylation signaling, respectively.

### Immunoblotting

Equal amounts of protein were boiled with sample buffer containing 10%  $\beta$ -mercaptoethanol (Sigma-Aldrich) at 95°C for 5 minutes, and 15  $\mu$ g protein of each sample mixture was loaded on 4% to 20% Criterion TGX (Bio-Rad, Hercules, CA) 26-well SDS-PAGE. Protein gels were transferred to mid-nitrocellulose membrane via Bio-Rad turbo-transfer for

14 minutes. Membranes were blocked with 5% nonfat dry milk in Tris-buffered saline containing 0.1% Tween 20 for 90 minutes at room temperature with gentle shaking. Primary antibodies were incubated in 5% nonfat dry milk in Tris-buffered saline containing 0.1% Tween 20 with gentle shaking overnight at 4°C. Secondary antibody (anti-rabbit-IgG-horseradish peroxidase or anti-mouse-IgG-horseradish peroxidase; 1:5000) incubations were performed in 5% nonfat dry milk in Tris-buffered saline containing 0.1% Tween 20 at room temperature for 90 minutes. Blots were developed with reagents from the Amersham ECL Western Blotting kit, and chemiluminescence signal was collected with Amersham Imager 600 System (ThermoFisher Scientific) and analyzed with the image analysis software Image J (National Institutes of Health). The primary antibodies and dilution were used as follows: anti-phosphorylated (Ser1177)-endothelial NO synthase (eNOS), 1:250 (Cell Signal No. 9570); anti-eNOS, 1:1000 (Cell Signal No. 32027); anti-phosphorylated (Ser473)-protein kinase B (AKT), 1:1000 (Cell Signal No. 9271S); anti-AKT, 1:1000 (Cell Signal No. 9272); anti-phosphorylated Smad 2, 1:1000 (Cell Signal No. 3108); anti-Smad2/3, 1:1000 (Cell Signal No. 3102); anti-transforming growth factor  $\beta$ 1 (TGF $\beta$ 1), 1:1000 (Cell Signal No. 3709); and anti-GAPDH, 1:1000 (Santa Cruz No. sc-32233).

### Echocardiography

Mice were lightly anesthetized with 1% to 2% isoflurane in a medical air/oxygen mixture during examinations and placed supine on a heated platform with electrocardiography leads. Core body temperature (monitored via rectal probe) was monitored via a rectal temperature probe with the animal on a heated circulating-water pad. Heart images were acquired using the Vevo2100 ultrasound system (VisualSonics, Toronto, ON, Canada) with a 30-MHz ultrasound probe (VisualSonics; MS-400 transducer).

### Telemetry

Telemetry was implanted into the mice. After a week of acclimation, we SC injected RELAX10 and monitored blood pressure and heart rate for a week. We found no change in these parameters.

### Histological Analysis

Cardiac fibrosis was evaluated using cross-section (midzone portion) of each heart stained with hematoxylin and eosin and/or Masson trichrome stain. Collagen-rich fibrotic regions were stained by Masson trichrome stain. The midzone portion of each heart was fixed with 10% formalin, followed with 100% ethanol. The paraffin-embedded sections were stained with routine hematoxylin and eosin and Masson trichrome staining

procedures. Briefly, slides were deparaffinized through xylenes and alcohols, stained with Mayer hematoxylin and eosin, dehydrated, and mounted with Permount. For Masson staining, slides were fixed with Bouin solution overnight, stained with Weiger iron hematoxylin and Biebrich scarlet-acid fuchsin, differentiated with phosphomolybdic-phosphotungstic acid, and transferred to aniline blue. After a brief wash, the slide was quickly dehydrated and mounted with Permount. Collagen content in each heart (apical portion) was measured via a total collagen assay kit from Quickzyme BioScience (the Netherlands).

### Statistical Analysis

Results are expressed as mean $\pm$ SE. To compare multiple groups, we performed the omnibus Kruskal-Wallis test. For all cases, the Kruskal-Wallis *P* value was  $\leq 0.01$ , suggesting that there is at least one difference among the various groups. For the comparison between vehicle and the groups, ISO and the groups, we used the Mann-Whitney *U* test. Differences were considered significant at  $P < 0.05$ , with *n* indicating the number of independent experiments or number of mice.

## Results

### Production and in Vitro Activity of RELAX10

The relaxin-2 peptide was cloned as a C-terminal fusion to wild-type Fc, then expressed in CHO G22 cells and purified as described in Materials and Methods. Analysis of the purified protein via mass spectrometry confirmed the purified protein (RELAX10) has the expected mass under reduced and nonreduced conditions (data not shown).

Using a cAMP assay as a simple screening assay, we found that RELAX10 was active in CHO cells overexpressing the relaxin-2 receptor, RXFP1, with an average half-maximal effective concentration value of 1.94 nmol/L (Figure 1A). It did not show activity in cell lines overexpressing related receptors (RXFP2, RXFP3, and RXFP4) or the assay control cell line (ADCYAP1R1) (Figure 2). The relaxin-2 peptide showed the same pattern of activity with an average half-maximal effective concentration of 0.106 nmol/L in RXFP1 overexpressing CHO cells and no activity on control cell lines (Figures 1A and 2). RELAX10 showed a 10- to 15-fold reduction in activity compared with the relaxin-2 peptide in the cAMP assay but retained specific signaling of the relaxin-2 receptor.

VEGF is a known downstream target of relaxin-2.<sup>6</sup> We further evaluated the activity of RELAX10 by examining its ability to stimulate the VEGF pathway in THP-1 cells. The relaxin-2 peptide increased VEGF transcripts, measured by using quantitative reverse transcription-polymerase chain reaction in THP-1 cells in a dose-dependent manner with a maximum detected increase of  $\approx 2.5$ -fold at 1.7 nmol/L

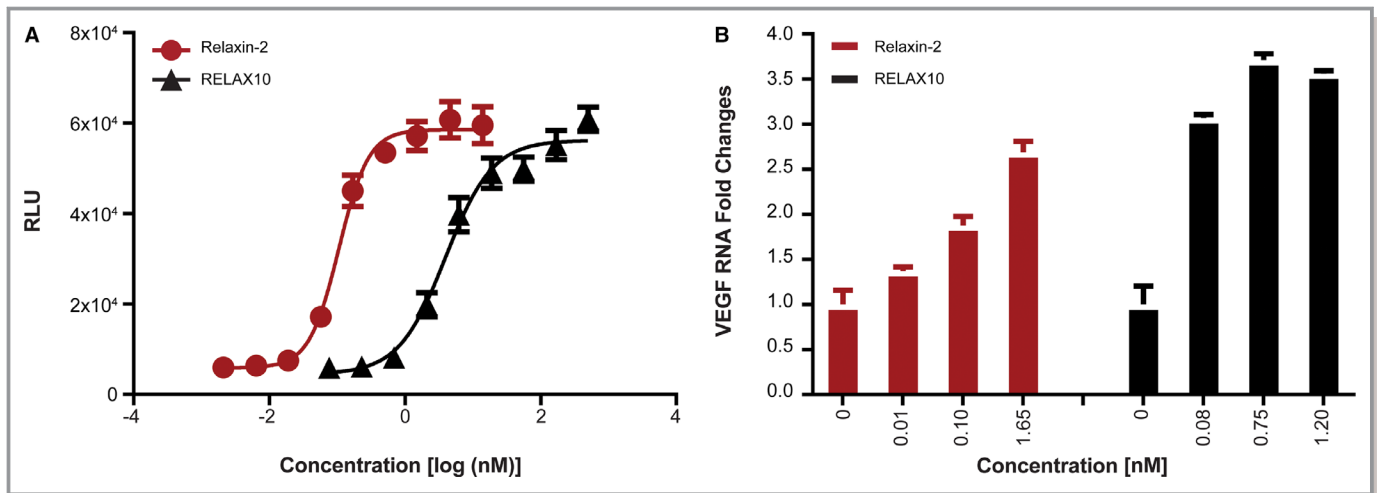


**Figure 1.** In vitro activity in relaxin/insulin-like family peptide receptor 1 (RXFP1) CHO and THP-1 cells. The in vitro activity of relaxin-2 and RELAX10 (a fusion protein composed of human relaxin-2 hormone and the Fc of a human antibody) was tested in human RXFP1-expressing CHO cells (CHO-K1 RXFP1 Gs) for the production of cAMP; relative light units (RLUs) represent the stimulation of cAMP production (A) or the stimulation of vascular endothelial growth factor (VEGF) transcripts in primary cell THP-1 (B). The relative fold change in VEGF mRNA level was calculated by the comparative Ct method using GAPDH expression for normalization. Results were calculated as fold changes over no treatment control. Multiple assays have been performed with the representative assay presented herein.

(Figure 1B). RELAX10 increased the levels of VEGF RNA 3- to 3.5-fold compared with control at concentrations ranging from 0.075 to 1.2 nmol/L (Figure 1B). No dose dependence was observed at the concentrations evaluated.

### Pharmacokinetic Profiles of RELAX10 in Rodents

Evaluation of the pharmacokinetic profile of RELAX10 in rodents showed that this Fc-peptide fusion has an extended half-life compared with the relaxin-2 peptide. The half-life of the human relaxin-2 peptide after intravenous administration is  $\approx 240$  minutes in humans<sup>24</sup> and 1.1 to 2 minutes in rodents.<sup>25</sup> RELAX10 was administered to Wistar rats by IV or SC routes at a dose of 4 mg/kg, followed by blood sample collection at various times after dosing. The in vivo pharmacokinetic profile of RELAX10 after either subcutaneous or intravenous administration in rats is shown in Figure 3A and 3B. After subcutaneous administration, peak plasma concentration was observed within 8 to 24 hours. The mean terminal half-life estimated from noncompartmental analysis was 3.59 and 3.75 days for the intravenous and subcutaneous dose groups, respectively, demonstrating an extended exposure with RELAX10 compared with relaxin-2 peptide.

The pharmacokinetic profile of RELAX10 was also evaluated in mice after administration of a single 6 mg/kg dose. The half-life observed was 5.58 and 7.06 days after intravenous or subcutaneous administration, respectively, demonstrating that the mean terminal half-life was  $\approx 26.5\%$  greater in the subcutaneous dose group compared with the intravenous dose group (Figure 3C). We also performed a dose escalation

pharmacokinetic study in mice to understand the relationship between the dose level and exposure as well as to provide data for dose selection for the in vivo functional studies. Figure 3D shows the mouse in vivo pharmacokinetic profile of RELAX10 after SC administration of 1, 6, or 30 mg/kg RELAX10, with peak serum concentration reached between 24 and 72 hours and a mean terminal half-life ranging from 4.59 to 7.06 days. The dose-normalized  $C_{max}$  (maximum concentration) decreased with an increasing dose. On the basis of the pharmacokinetic simulation (data not shown), an SC injection of 30 mg/kg once per week for 2 weeks was chosen for drug administration in the in vivo studies.

### Activity of RELAX10 in Models of Hypertrophy and Fibrosis

It was shown previously that sustained delivery of relaxin-2 via minipump prevents cardiac remodeling and fibrosis in a mouse model of isoproterenol-induced cardiomyopathy.<sup>13</sup> We wanted to determine whether RELAX10 could also prevent or attenuate cardiac remodeling in the same model. On the basis of a pilot study, we found that a dose of 15 mg/kg per day isoproterenol delivered via minipump for 14 days was appropriate to induce cardiac hypertrophy and fibrosis, and that coadministration of enalapril, an angiotensin-converting enzyme inhibitor, at 25 mg/kg per day ameliorated this increase in hypertrophy and fibrosis (Figure 4A). Figure 5 shows that this dose of isoproterenol treatment leads to an increase in the ratio of HW/BW and HW/TL compared with vehicle-treated mice. As shown in Figure 5A and 5B, the

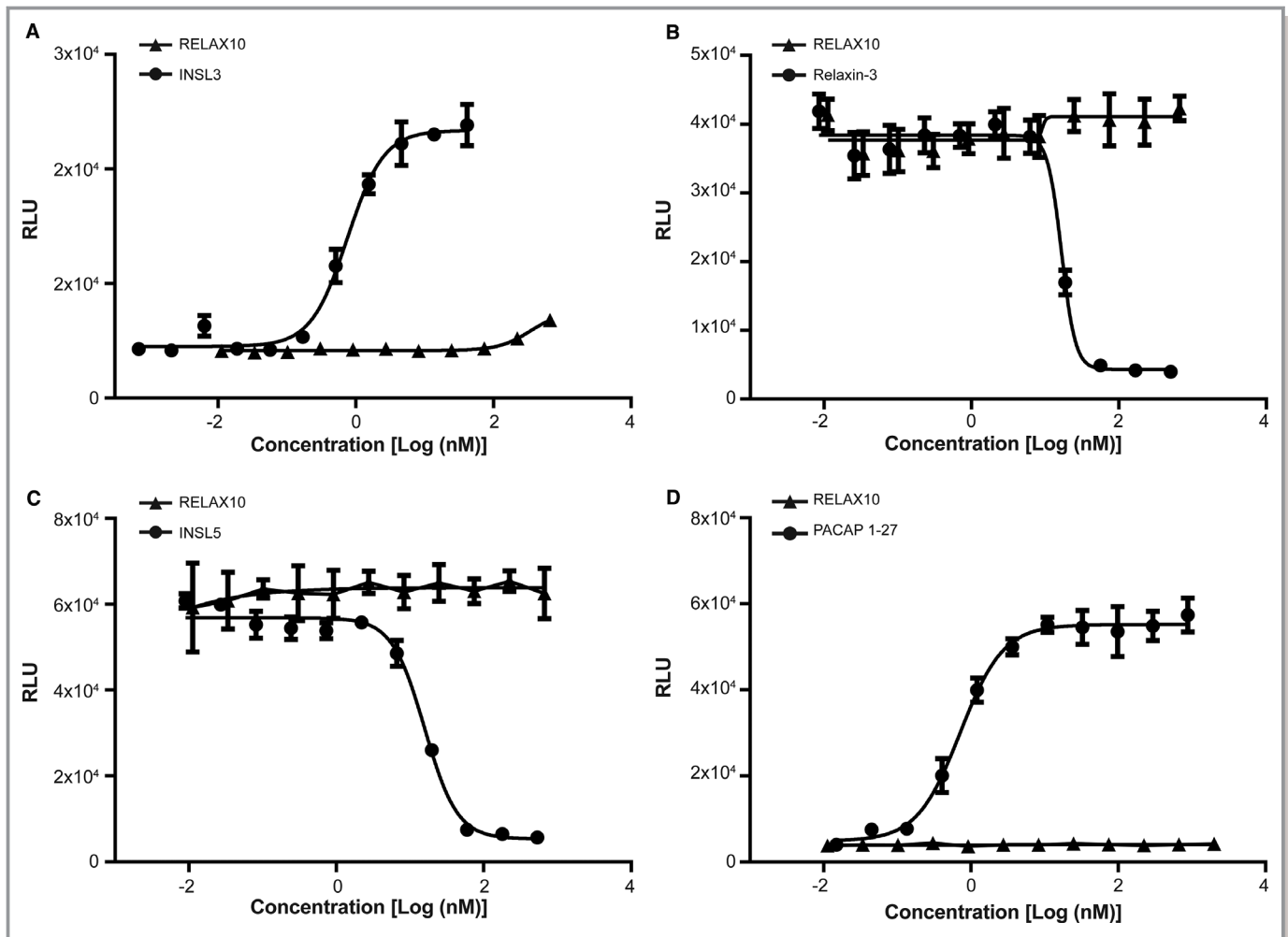


**Figure 2.** In vitro specificity in relaxin/insulin-like family peptide receptor 2 (RXFP2) (A), RXFP3 (B), RXFP4 (C), or ADCYAP1R1 (D) CHO cells. The in vitro specificity of RELAX10 was tested in human RXFP2-, RXFP3-, RXFP4-, or ADCYAP1R1-expressing CHO cells for the stimulation or inhibition of cAMP production; relative light units (RLUs) represent the cAMP concentration. cAMP assays were performed as described for RXFP1 cell line, except for cell lines RXFP3 and RXFP4, in which 25 or 20  $\mu\text{mol/L}$  forskolin (R&D Systems), respectively, was added to the dilution plate and serum-free medium to increase intracellular levels of cAMP as the ligands used in the assay will inhibit cAMP production. INSL3 (RXFP2), relaxin-3 (RXFP3), INSL5 (RXFP4), and PACAP1-27 (ADCYAP1R1) were used as positive controls. Experiments were performed at least twice.

increase in cardiac hypertrophy observed with isoproterenol was significantly attenuated when isoproterenol was administered concomitantly with enalapril, relaxin-2 peptide, or RELAX10. The relaxin-2 peptide has been previously shown to reduce adverse remodeling,<sup>13</sup> and this is confirmed by our results.

Consistent with increased cardiac hypertrophy after isoproterenol treatment, cardiac function (ie, ejection fraction and fractional shortening), as measured by echocardiography, was significantly decreased in isoproterenol-treated animals (Figure 5C and 5D). Cotreatment of enalapril with isoproterenol led to a significant improvement in contractile function, approaching that of the vehicle control level (Figure 5C and 5D), whereas there was a trend toward improvement of contractile function by cotreatment with either RELAX10 or

relaxin-2 peptide (Figure 5C and 5D). These changes in cardiac function are consistent with the antihypertrophic effects of RELAX10, relaxin-2 peptide, or enalapril.

The effects of these treatments on cardiac fibrosis were assessed by histological evaluation of heart slices using Masson trichrome staining. Figure 5E shows staining of representative hearts from vehicle (a), vehicle+RELAX10 (b), isoproterenol (c), and isoproterenol+RELAX10 (d) treated animals. Two weeks of treatment with isoproterenol leads to increased fibrosis (indicated by the blue color) compared with vehicle alone. As shown in Figure 5F, there was a significant increase in collagen in isoproterenol-treated hearts, which was attenuated by coadministration of RELAX10, relaxin-2 peptide, or enalapril. Taken together, the data show that RELAX10 reduces fibrosis and hypertrophy induced by isoproterenol.

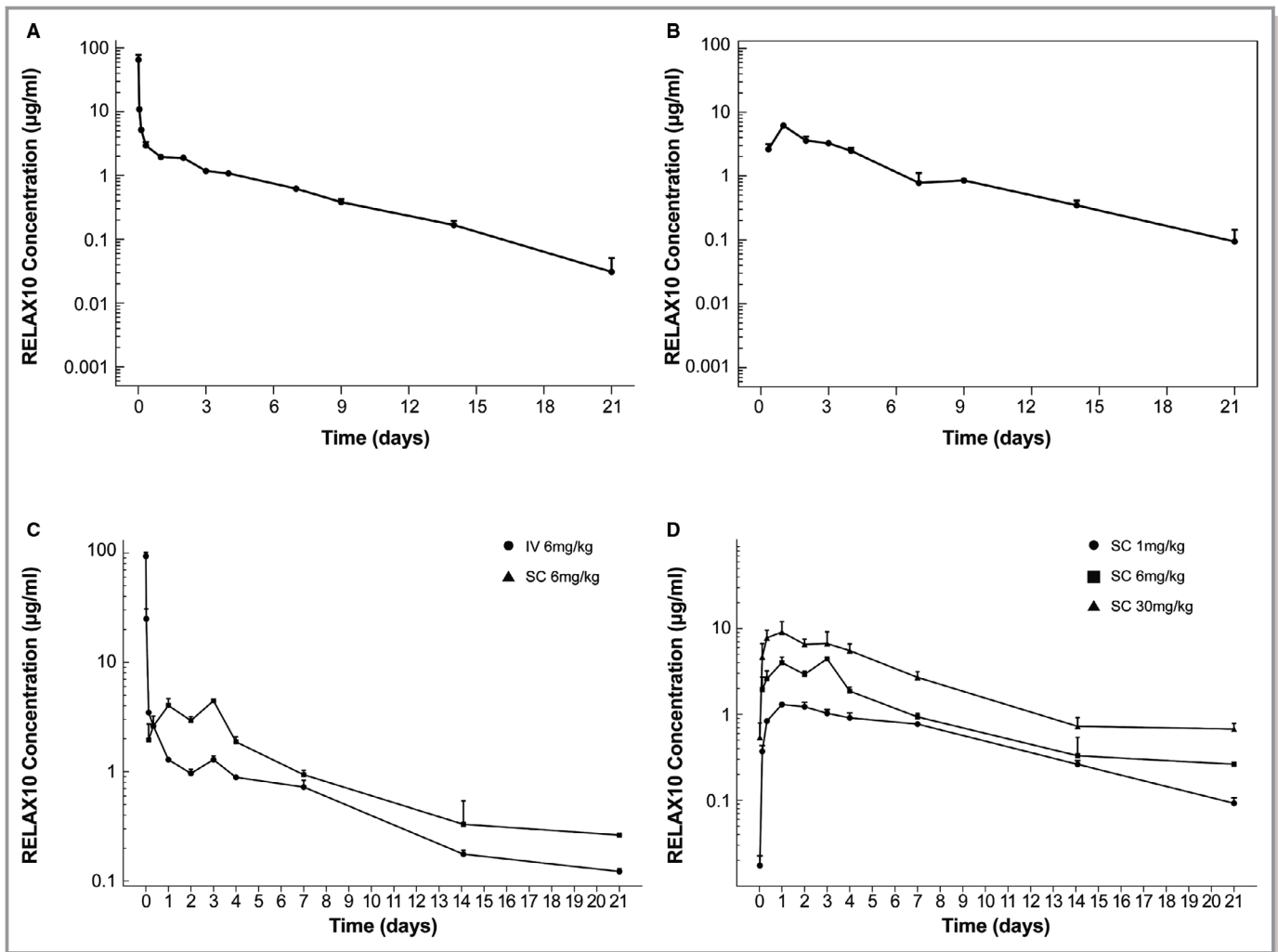


**Figure 3.** Pharmacokinetic profiles in rodent. The in vivo pharmacokinetic profiles of RELAX10 in rats was shown after intravenous (A) and subcutaneous (B) administration. The dose used for the rat pharmacokinetic study is 4 mg/kg, and blood sample collection occurs at various times after dosing. C, The pharmacokinetic profile of RELAX10 was also evaluated in mice after administration of a single 6 mg/kg dose by either IV or SC administration. D, A subcutaneous administration dose escalation pharmacokinetic study in mice to understand the relationship between the dose level and exposure. All the samples were tested by ELISA, in which an anti-Fc monoclonal antibody TM446 (AstraZeneca) was used to coat the ELISA plate. The horseradish peroxidase (HRP)-conjugated polyclonal antibody from the Relaxin-2 detection ELISA kit (R&D Systems) was used as the ELISA detection reagent.

### RELAX10 Treatment Increased Myocardial NO/S-Nitrosylation Signaling

RXFP1 is a major G-protein-coupled receptor for relaxin-2.<sup>6,26</sup> This receptor is expressed not only in reproductive tissues, but also in nonreproductive tissues, including vascular endothelial cells, smooth muscle cells, and cardiomyocytes.<sup>26,27</sup> The vascular actions of relaxin-2 are mediated mainly through NO vasodilator pathways.<sup>28</sup> It has been also shown that serelaxin attenuates myocardial infarction after ischemia/reperfusion injury via an eNOS-dependent mechanism.<sup>29,30</sup>

The canonical eNOS signaling pathway involves G-protein-coupled receptor-mediated activation of AKT, which, in turn,

activates eNOS by phosphorylation at Ser-1177.<sup>31</sup> As shown in Figure 6A and 6B, treatment with RELAX10 alone significantly increased the ratio of phosphorylated (Ser1177)-eNOS/total eNOS and phosphorylated (Ser473)-AKT/total AKT. It is not surprising that isoproterenol also led to a comparable activation of AKT/eNOS pathway because isoproterenol treatment leads to an increase of intracellular  $Ca^{2+}$  and the activity of eNOS is  $Ca^{2+}$  dependent.<sup>32</sup> Interestingly, cotreatment of isoproterenol and RELAX10 elicited an additive increase of eNOS activity (Figure 6A). However, there was no additive increase in phosphorylation of eNOS with isoproterenol and enalapril cotreatment, suggesting that enalapril, which acts via inhibition of angiotensin-converting enzyme signaling, does not per se enhance eNOS phosphorylation.

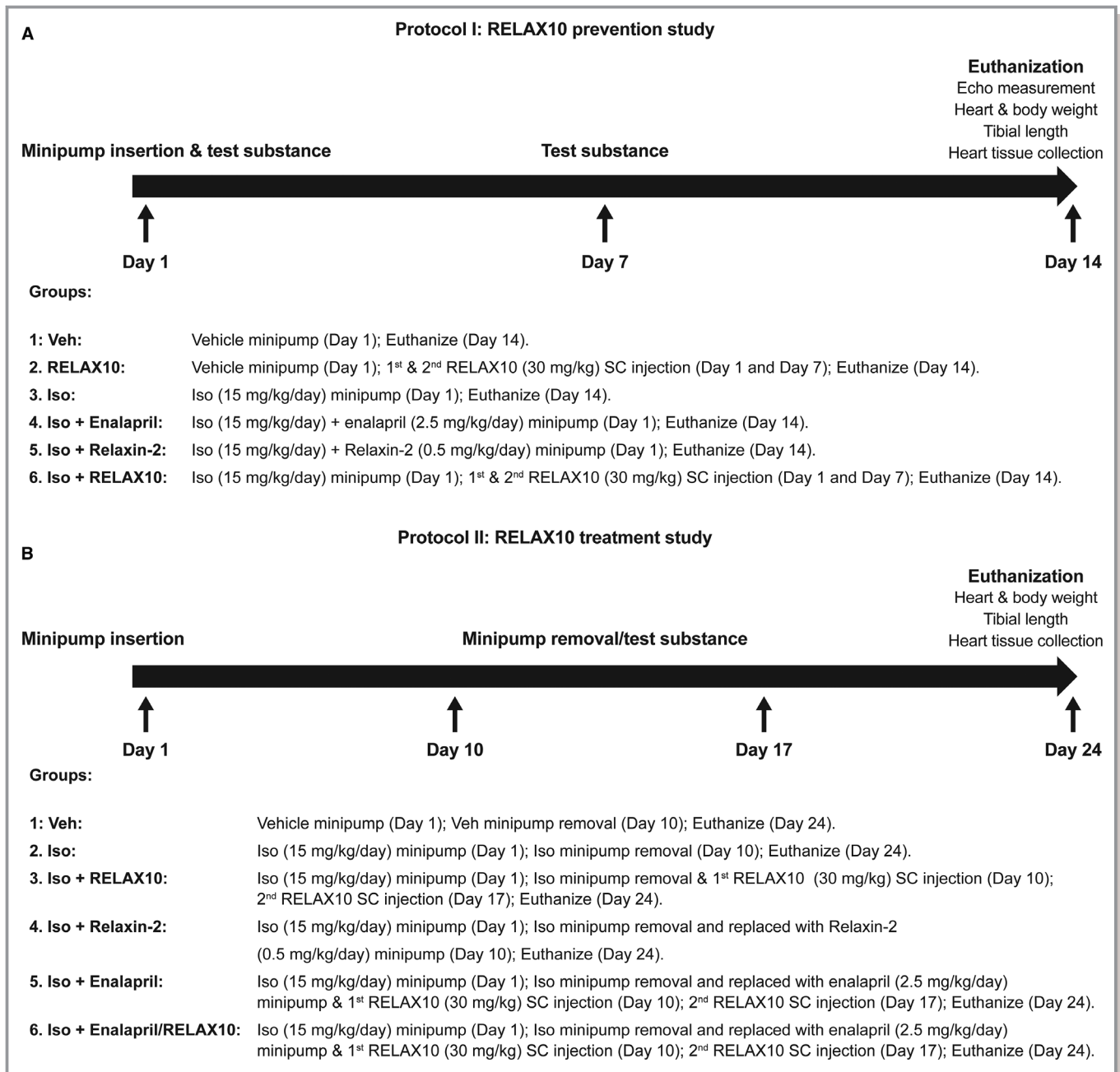


**Figure 4.** Protocol for RELAX10 prevention study (A) and treatment study (B). Veh indicates vehicle control.

Our previous studies<sup>22,23,33–36</sup> have demonstrated that NO can directly modify protein sulfhydryl residues through protein S-nitrosylation, which has emerged as an important post-translational protein modification in cardiovascular signaling and cardioprotection.<sup>37–39</sup> Having determined that relaxin-2 or RELAX10 treatment leads to activation of AKT/eNOS signaling, we examined whether 2 weeks of RELAX10 administration would also alter protein S-nitrosylation in the heart. Protein S-nitrosylation was measured in heart homogenates by a modified biotin switch method using CyDye-maleimide

monoreactive fluorescence dyes.<sup>21,22</sup> After the S-nitrosylation/dye switch, equal amounts of each individual sample labeled with a different dye (Cy3 in Figure 6C and Cy5 in Figure 6D) were combined (Figure 6E) and separated by nonreducing gel electrophoresis in the dark. As shown in Figure 6F, either RELAX10 or isoproterenol treatment alone led to a modest comparable increase in protein S-nitrosylation, whereas cotreatment with RELAX10 and isoproterenol provided an additive increase in the NO/S-nitrosylation signaling.

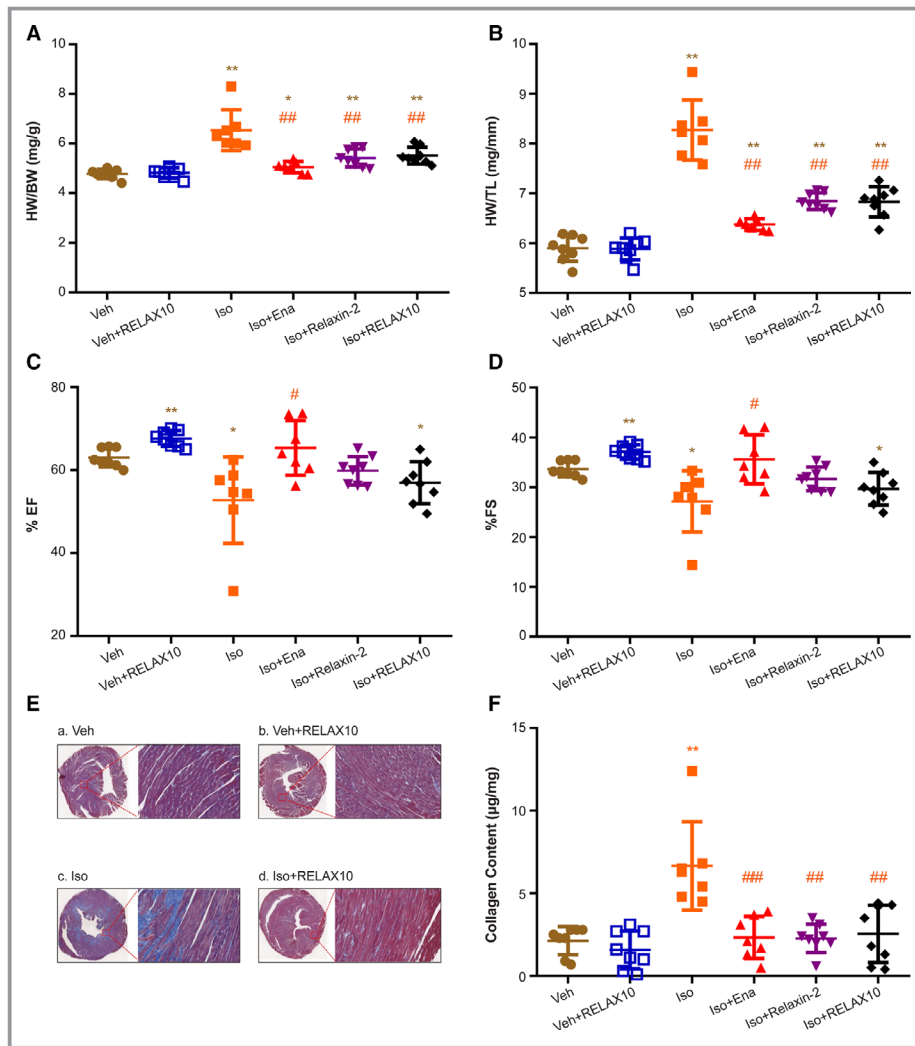


**Figure 5.** Heart weight (HW)/body weight (BW), HW/tibial length (TL), echocardiographic results, and Masson staining for fibrosis and collagen content of RELAX10 prevention study. On the day of treatment termination, mice were euthanized and HW, BW, and TL were measured. Results of HW/BW (**A**) and HW/TL (**B**) are expressed as mean±SE. Cardiac function (ie, percentage of ejection fraction [EF; **C**] and fractional shortening [FS; **D**]) of each heart was measured by echocardiography. **E**, A representative Masson staining image of cardiac cross-section was shown from each group (n=8). Compared with vehicle control (a) or RELAX10-treated (b) alone, isoproterenol treatment (c) led to an increase in fibrosis (indicated by the blue color in each enlarged inset). Coadministration of RELAX10 and isoproterenol (d) largely attenuated isoproterenol-induced fibrosis. **F**, Collagen content in each heart (apical portion, ≈20–30 mg) was measured via a total collagen assay kit from Quickzyme BioScience (the Netherlands). Statistical significance was determined using a Kruskal-Wallis test, followed by the Mann-Whitney *U* test, to compare with vehicle control (Veh) or isoproterenol group (n=8 in each group). \**P*<0.05, \*\**P*<0.01 vs Veh group. #*P*<0.05, ##*P*<0.01 vs isoproterenol group.

### Antifibrotic Signaling Pathway Involved in RELAX10-Induced Antifibrotic Effect

Consistent with the relaxin-2 peptide study by Samuel et al,<sup>13</sup> the antihypertrophic and antifibrotic effect of RELAX10 in preventing isoproterenol-induced fibrosis progression was associated with downregulation of TGFβ1 expression (Figure 6G)

and phosphorylation of Smad2 (Figure 6H). As shown in Figure 6G, isoproterenol treatment significantly increased the expression of TGFβ1, whereas cotreatment with RELAX10, relaxin-2 peptide, or enalapril greatly attenuated the isoproterenol-induced TGFβ1 expression. Isoproterenol treatment also showed a trend toward increased phosphorylation of Smad2, a major downstream target of TGFβ1 signaling, as indicated by

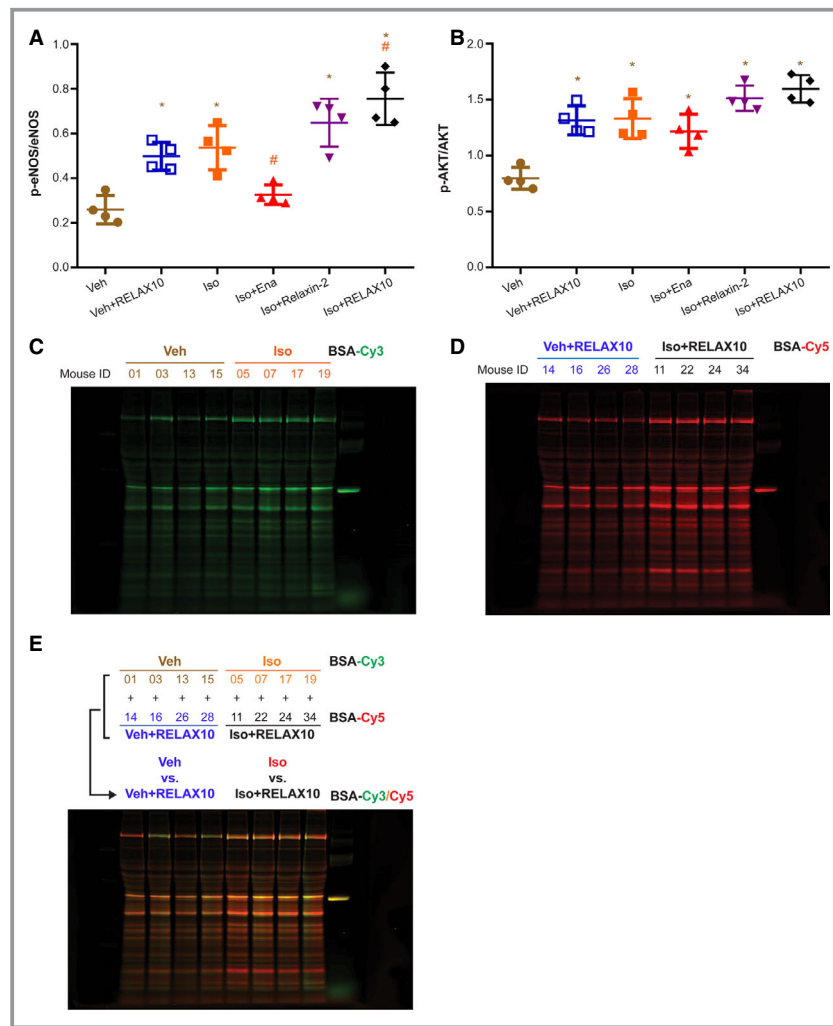


**Figure 6.** Phosphorylated protein kinase B (p-AKT)/AKT, phosphorylated endothelial NO synthase (p-eNOS)/eNOS, transforming growth factor  $\beta$  1 (TGF $\beta$ 1)/GAPDH, and phosphorylated Smad (p-Smad) 2/Smad Western blot results and S-nitrosylation signaling of RELAX10 prevention study. The basal portion of heart (4 randomly picked from 8 hearts in each group) was subjected for heart homogenate preparation. Heart samples were collected at day 14. Equal amounts of sample were subjected to SDS-PAGE and immunoblot, as described in Materials and Methods. The ratios of anti-p-eNOS/eNOS (**A**) and p-AKT/AKT (**B**) were assessed by band densitometry, with statistical significance as shown in each figure ( $n=4$  in each group).  $*P<0.05$  vs vehicle control (Veh) group.  $\#P<0.05$  vs isoproterenol group. Aliquots of same heart homogenate for immunoblot experiment were subjected to a modified biotin switch method using sulfhydryl-mono-reactive CyDye-maleimide fluors. After labeling, equal amount of Cy3-maleimide- and Cy5-maleimide-labeled S-nitrosylation proteins from 2 samples (Veh vs Veh+RELAX10 or isoproterenol vs isoproterenol+RELAX10) were combined and subjected to nonreducing SDS-PAGE in the dark. On the basis of the standardized BSA-S-nitrosylation equal fluorescence intensity for each labeled dye, the fluorescence image of Cy3 (**C**) or Cy5 (**D**) maleimide dyes was scanned and Cy3/Cy5 overlaid (**E**) using a Li-Cor Odyssey scanner at 700 and 800 nm, respectively. **F**, Statistical significance shown in the figure was analyzed by the ratio of the fluorescence intensity of whole lane for each paired 2 samples ( $n=4$ ).  $*P<0.05$  vs Veh group.  $\#P<0.05$  vs isoproterenol or Veh+RELAX10. Statistical significance was determined using a Kruskal-Wallis test, followed by the Mann-Whitney  $U$  test, to compare with Veh or isoproterenol group. The ratios of anti-TGF $\beta$ 1/GAPDH (**G**) and anti-p-Smad2/Smad (**H**) were analyzed by band densitometry, with statistical significance as shown in the figure.  $*P<0.05$  vs Veh group.  $\#P<0.05$  vs isoproterenol group.

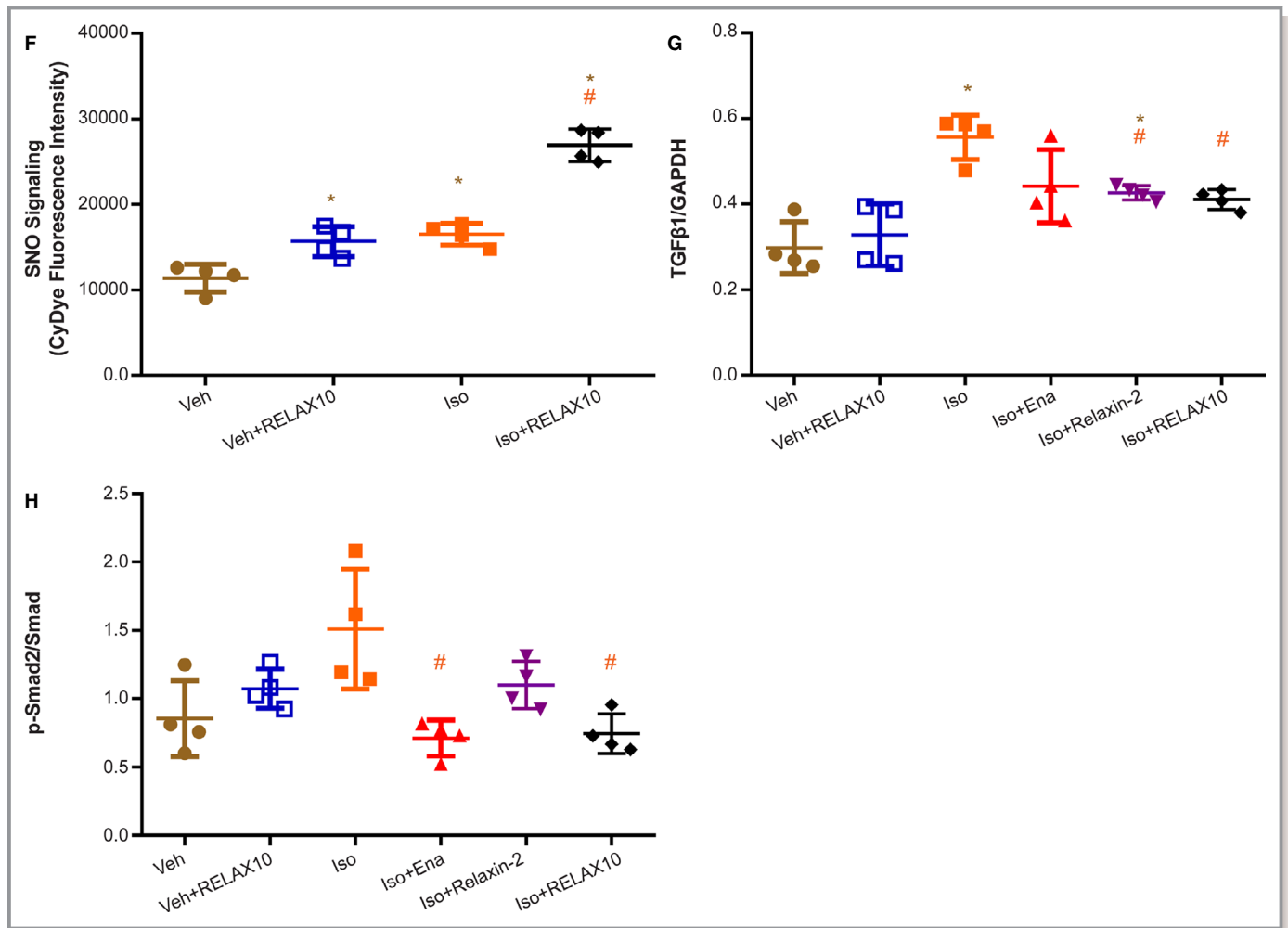


**Figure 6.** Continued.

the increased ratio of phosphorylated Smad2/Smad (Figure 6H). Two weekly subcutaneous injections of RELAX10 significantly reduced phosphorylated Smad2/Smad ratio to levels similar to that of the vehicle control. Thus, similar to the effect of relaxin-2, RELAX10 disrupts TGFβ1 signal transduction in the heart by inhibiting the phosphorylation of Smad2.<sup>14</sup>

### Treatment With RELAX10 Reverses Isoproterenol-Induced Cardiac Hypertrophy and Fibrosis

To investigate whether RELAX10 could also reverse established cardiac hypertrophy and fibrosis in the isoproterenol model, we administered isoproterenol for 10 days and then stopped the isoproterenol treatment and tested whether a subsequent 14-day treatment with RELAX10, relaxin-2, or enalapril would reverse remodeling. As shown in Figure 4B, 6 groups (8 mice in each group) were used to study the treatment effect of RELAX10 together with comparison to the treatments of relaxin-2 peptide alone and the combination of RELAX10 and enalapril.

Ten days of isoproterenol treatment significantly increase the ratio of HW/BW and HW/TL, demonstrating an increase in hypertrophy in isoproterenol-treated mice compared with vehicle (Figure 7A and 7B). The isoproterenol-induced hypertrophy was not reversed without treatment as the mice treated with isoproterenol for 10 days, followed by 14 days with no treatment, have an increased HW/BW, HW/TL (Figure 7A and 7B), and collagen content (Figure 7C) compared with the vehicle control. The increase in cardiac hypertrophy initiated by isoproterenol treatment was significantly attenuated by posttreatment with RELAX10, or relaxin-2 peptide, with levels observed similar to the vehicle control (Figure 7A and 7B). In addition, the isoproterenol-induced increase in collagen was blocked by treatment with RELAX10, relaxin-2 peptide, or enalapril (Figure 7C). Consistent with the data in the prevention study, in the treatment study, RELAX10 led to an increase in AKT/eNOS signaling (Figure 8A and 8B) and a decrease in isoproterenol-induced TGFβ1/Smad2 signaling (Figure 8C and 8D).

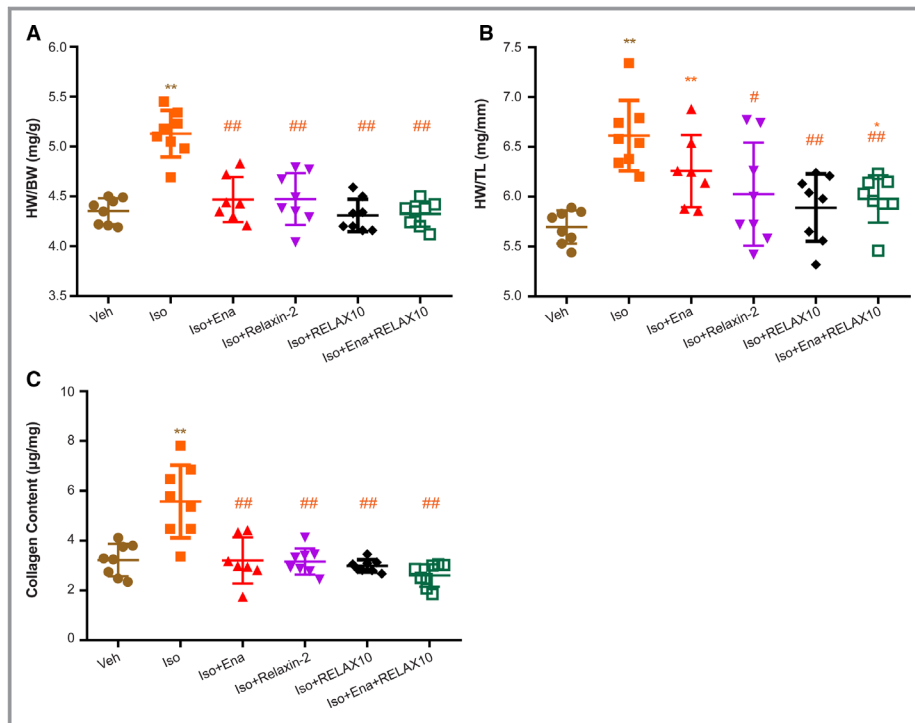


**Figure 7.** Heart weight (HW)/body weight (BW), HW/tibial length (TL), and collagen content of RELAX10 treatment study. On the day of treatment termination, mice were euthanized and HW, BW, and TL were measured. Results of HW/BW (A), HW/TL (B), and collagen content (C) are expressed as mean±SE. Statistical significance was determined using a Kruskal-Wallis test, followed by the Mann-Whitney *U* test, to compare with vehicle control (Veh) or isoproterenol group. n=8 in each group. \**P*<0.05, \*\**P*<0.01 vs Veh group. #*P*<0.05, ##*P*<0.01 vs isoproterenol group.

## Discussion

The relaxin-2 peptide signaling pathways have been extensively studied, and administration of the peptide in animal models has resulted in pleiotropic cardiovascular effects, including reductions in cardiac hypertrophy and fibrosis.<sup>4,6,8</sup> In addition, intravenous administration of a recombinant form of the peptide, serelaxin, for 48 hours in patients with acute HF led to improvement in markers of cardiac, renal, and hepatic damage and reduced congestion, but the effects diminished rapidly on treatment termination.<sup>11</sup> We hypothesized that the transient treatment benefits could be because of the limited treatment duration and short half-life of serelaxin because continuous infusion of relaxin-2 peptide using subcutaneously implanted minipump has resulted in long-term benefits in animal studies.<sup>14–16</sup> This hypothesis is also supported by the *in vitro* studies demonstrating that serelaxin exerted both short- and long-term changes in vascular cells.<sup>4,8</sup> We developed a molecule, RELAX10, with extended half-life and evaluated it *in vitro* and *in vivo* to determine if it can positively impact cardiac hypertrophy and fibrosis, which are characteristics of both HF with preserved ejection fraction and HF with reduced ejection fraction.

*In vitro* RELAX10 demonstrated the expected specificity and ability to signal, although the activity was found to be slightly reduced compared with the relaxin-2 peptide. We found that RELAX10 had a terminal half-life of 7 and 3.75 days in mice and rats, respectively, after subcutaneous administration. This half-life represented a step change compared with the reported half-life of 240 minutes for serelaxin in humans<sup>24</sup> and presented an opportunity to study the impact of extended dosing on key characteristics of HF, including cardiac hypertrophy and fibrosis.

We began our studies by examining if RELAX10 could prevent isoproterenol-induced cardiac hypertrophy and fibrosis in mice. As a positive control, we used enalapril, an angiotensin-converting enzyme inhibitor, as a study performed by Samuel et al showed it to be an effective treatment to inhibit fibrosis progression in mice.<sup>13</sup> In the prevention study, RELAX10 was able to significantly reduce the isoproterenol-induced cardiac hypertrophy and fibrosis and demonstrated a trend toward improvement of cardiac function, as measured by ejection fraction and fractional shortening. RELAX10 had a comparable effect on hypertrophy, fibrosis, and cardiac function as that induced by continuously delivered relaxin-2 peptide, demonstrating that, although the fusion protein had

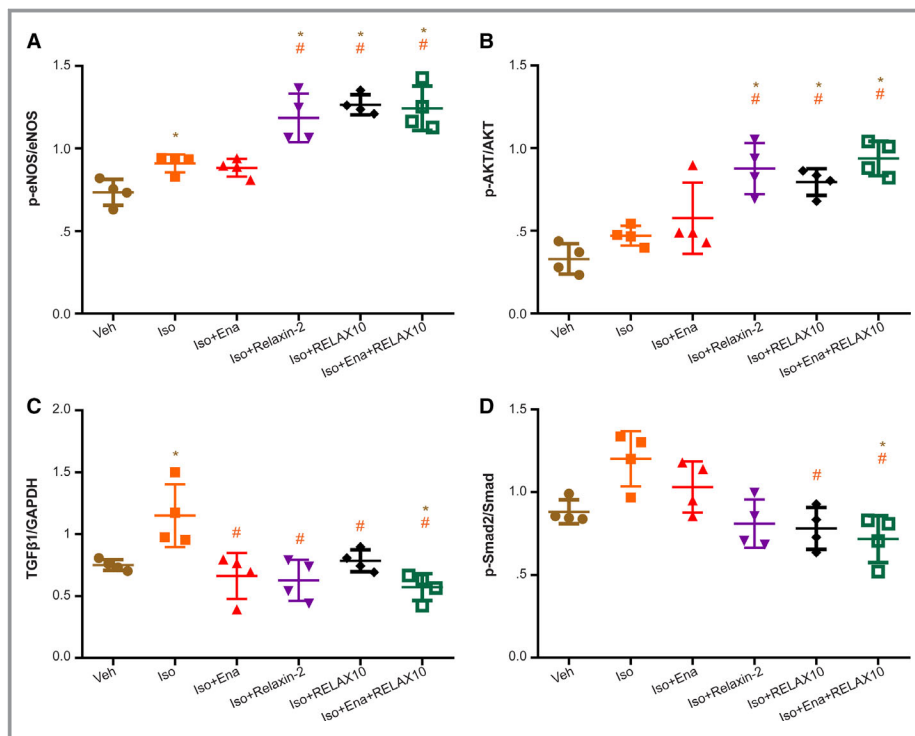


**Figure 8.** Phosphorylated protein kinase B (p-AKT)/AKT, phosphorylated endothelial NO synthase (p-eNOS)/eNOS, transforming growth factor  $\beta$ 1 (TGF $\beta$ 1)/GAPDH, and phosphorylated Smad (p-Smad) 2/Smad Western blot results of RELAX10 treatment study. The basal portion of heart (4 randomly picked from 8 hearts in each group) was subjected for heart homogenate preparation. Heart samples were collected at day 24. Equal amounts of sample were subjected to SDS-PAGE and immunoblot, as described in Materials and Methods. The ratios of anti-p-eNOS/eNOS (A), p-AKT/AKT (B), anti-TGF $\beta$ 1/GAPDH (C), and anti-p-Smad2/Smad (D) were assessed by band densitometry with statistical significance, as shown in each figure (n=4 in each group). Statistical significance was determined using a Kruskal-Wallis test, followed by the Mann-Whitney U test, to compare with vehicle control (Veh) or isoproterenol group. \* $P$ <0.05 vs Veh group. # $P$ <0.05 vs isoproterenol group.

slightly reduced in vitro potency, the in vivo activity matched that of the recombinant peptide. Coadministration of enalapril led to antihypertrophic and antifibrotic effects as well as significant improvement in cardiac function. Coadministration of isoproterenol with RELAX10 led to attenuation in the isoproterenol-induced activation of the TGF $\beta$ 1/Smad2 signaling pathways. Interestingly, from the point of view of signaling pathways, coadministration of isoproterenol with RELAX10 or the relaxin-2 peptide activates the eNOS/NO signaling, whereas with enalapril, it does not (Figure 6A).

It has been reported that relaxin-2 deficiency leads to collagen deposition and organ fibrosis,<sup>40–42</sup> whereas relaxin-2 treatment reduces collagen production and reverses cardiac fibrosis.<sup>13,14</sup> We evaluated whether RELAX10 could reverse isoproterenol-induced cardiac damage by administering the molecule after the damage was inflicted. This was important as it more closely resembles the target population, as individuals will be identified once the hypertrophy and fibrosis has been established, leading to the impairment of cardiac function. Ten

days of isoproterenol treatment significantly increases myocardial collagen content and increases myocardial interstitial fibrosis. Postisoproterenol treatment with RELAX10, relaxin-2 peptide, or enalapril led to a significant decrease in isoproterenol-induced hypertrophy and the isoproterenol-induced increase in collagen, resulting in levels similar to vehicle control.

The antifibrotic effects of relaxin-2 have been well studied in the context of cardiac disease. Relaxin-2 activates several signaling cascades that have been shown to be beneficial in the setting of ischemia-reperfusion and HF.<sup>4,43,44</sup> Relaxin-2 has been shown to activate the NO signaling pathway and mediate beneficial signaling against oxidative stress during hypertrophy and HF.<sup>28,45</sup> Interestingly, a recent study suggests that relaxin-2-mediated inhibition of TGF $\beta$ 1/Smad2 phosphorylation signal transduction is also dependent on NO.<sup>46</sup> This might not be surprising as it was shown more than a decade ago that the endothelial NO/cGMP/PKG (Protein Kinase G) pathway interferes with TGF $\beta$ 1/Smad2 signaling by directing the proteasomal degradation of activated Smad.<sup>47</sup> In addition to activating

soluble guanylyl cyclase/cGMP/PKG signaling pathways, NO-mediated protein S-nitrosylation has been recently shown to play an essential role in the cardiovascular system.<sup>37–39,48–51</sup> Therefore, we evaluated S-nitrosylation signaling in RELAX10-treated cardiac tissue by a modified biotin switch method using sulfhydryl-mono-reactive CyDye-maleimide fluoros. As shown in Figures 6C–6F, RELAX10 treatment alone slightly but significantly increased S-nitrosylation signaling, which is consistent with its effect on the activation of AKT/eNOS signaling pathway. Interestingly, cotreatment with RELAX10 and isoproterenol lead to an almost 2-fold increase in protein S-nitrosylation. On the basis of the literature, NO/S-nitrosylation signaling might be also involved in regulating fibrosis development. For example, nuclear translocation of CLIC4 (chloride intracellular channel protein) is essential for its role in Ca<sup>2+</sup> and stress-induced TGFβ signaling involving apoptosis and differentiation. Malik et al have shown that S-nitrosylation of CLIC4 facilitates its nuclear translocation, where it enhances TGFβ1 by protecting phosphorylated Smad2/3 from dephosphorylation.<sup>52</sup> Of interest, Menazza et al found a decrease in S-nitrosylation of CLIC4 in failing human hearts.<sup>53</sup> However, the mechanism responsible and whether it is compensatory or involved in HF are unclear. Irwin et al have reported a potential role for S-nitrosylation in NO-mediated inhibition of platelet adhesion to collagen.<sup>54</sup> In addition, other fibrotic players, such as matrix metalloproteinase and tissue transglutaminase, have been also demonstrated to be regulated by NO/S-nitrosylation signaling.<sup>55,56</sup>

Cardiac fibrosis is a pathological feature present in heart disease, such as myocardial infarction, cardiomyopathies, and HF. Unfortunately, currently, there are few effective treatments to block the progression of cardiac fibrosis. These findings provide strong support for RELAX10 in the treatment of hypertrophy and fibrosis and suggest that it might provide benefits to patients with HF. These data also show that RELAX10 and enalapril activate different signaling pathways, suggesting that combined treatment might have added benefits.

## Acknowledgments

We would like to thank Diana Pao, Judy Patterson, and Monika Papworth for their contributions to the program. We thank Steven Novick for help with the statistical analysis. We thank the National Heart, Lung, and Blood Institutes/National Institutes of Health Animal Surgery and Resources Core for their assistance. Support for figures was provided by Sepidah Farshadi of the Compass Group, working on behalf of AstraZeneca.

All authors contributed to the research, edited, and approved the manuscript. Dr Sun, Dr Hao, Dr Murphy, and Dr Walker supervised all aspects of the work. Dr Osbourn and Dr Karathanasis provided guidance and intellectual input. Dr Sun, Dr Fillmore, H. Ma, Dr Springer, Dr Yu, A. Sadowska, A. Garcia, R. Chen, V. Muniz-Medina, K. Rosenthal, J. Lin, and Dr Hao performed the experiments. Dr Sun, Dr Kuruvilla, Dr Hao, Dr Karathanasis, Dr Walker, and Dr Murphy

provided input into the design of the experiments. Dr Sun, Dr Hao, Dr Fillmore, H. Ma, Dr Springer, Dr Yu, A. Sadowska, A. Garcia, R. Chen, V. Muniz-Medina, K. Rosenthal, J. Lin, Dr Kuruvilla, Dr Karathanasis, Dr Walker, and Dr Murphy analyzed and interpreted the data. All data related to this study are in the article.

## Sources of Funding

This work was supported by National Heart, Lung, and Blood Institute Intramural Fund (Dr Murphy) and a CRADA (Cooperative Research and Development Agreements) from MedImmune/AstraZeneca.

## Disclosures

Dr Hao, A. Sadowska, A. Garcia, R. Chen, V. Muniz-Medina, K. Rosenthal, J. Lin, and Dr Kuruvilla are employees of AstraZeneca and have stock and/or stock options or interests in AstraZeneca. Dr Osbourn, Dr Karathanasis, and Dr Walker were employees of AstraZeneca at the time of the study and manuscript submission. The remaining authors have no disclosures to report.

## References

- Lam C, Lyass A, Kraigher-Krainer E, Massaro J, Lee D, Ho J, Levy D, Redfield M, Pieske B, Benjamin E, Vasan R. Cardiac dysfunction and noncardiac dysfunction as precursors of heart failure with reduced and preserved ejection fraction in the community. *Circulation*. 2011;124:24–30.
- Ponikowski P, Anker SD, AlHabib KF, Cowie MR, Force TL, Hu S, Jaarsma T, Krum H, Rastogi V, Rohde LE, Samal UC, Shimokawa H, Budi Siswanto B, Sliwa K, Filippatos G. Heart failure: preventing disease and death worldwide. *ESC Heart Fail*. 2014;1:4–25.
- Mozaffarian D, Benjamin EJ, Go AS, Arnett DK, Blaha MJ, Cushman M, Ferranti S, Després J-P, Fullerton HJ, Howard VJ, Huffman MD, Judd SE, Kissela BM, Lackland DT, Lichtman JH, Lisabeth LD, Liu S, Mackey RH, Matchar DB, McGuire DK, Mohler ER, Moy CS, Muntner P, Mussolino ME, Nasir K, Neumar RW, Nichol G, Palaniappan L, Pandey DK, Reeves MJ, Rodriguez CJ, Sorlie PD, Stein J, Towfighi A, Turan TN, Virani SS, Willey JZ, Woo D, Yeh RW, Turner MB. Heart disease and stroke statistics—2015 update: a report from the American Heart Association. *Circulation*. 2015;131:e29–e322.
- Sarwar M, Du XJ, Dschietzig TB, Summers RJ. The actions of relaxin on the human cardiovascular system. *Br J Pharmacol*. 2017;174:933–949.
- Bathgate RAD, Kocan M, Scott DJ, Hossain MA, Good SV, Yegorov S, Bogerd J, Gooley PR. The relaxin receptor as a therapeutic target—perspectives from evolution and drug targeting. *Pharmacol Ther*. 2018;187:114–132.
- Xiao J, Huang Z, Chen CZ, Agoulnik IU, Southall N, Hu X, Jones RE, Ferrer M, Zheng W, Agoulnik AI, Marugan JJ. Identification and optimization of small-molecule agonists of the human relaxin hormone receptor RXFP1. *Nat Commun*. 2013;4:1953.
- Ghosh RK, Banerjee K, Tummala R, Ball S, Ravakha K, Gupta A. Serelaxin in acute heart failure: most recent update on clinical and preclinical evidence. *Cardiovasc Ther*. 2017;35:55–63.
- Ghulam M, Adeel S, Izhar H. Recent progress in the therapeutic role of serelaxin in vascular dysfunction. *Curr Protein Pept Sci*. 2018;19:1079–1087.
- Unemori E. Serelaxin in clinical development: past, present and future. *Br J Pharmacol*. 2017;174:921–932.
- Teerlink JR, Cotter G, Davison BA, Felker GM, Filippatos G, Greenberg BH, Ponikowski P, Unemori E, Voors AA, Adams KF, Dorobantu MI, Grinfeld LR, Jondeau G, Marmor A, Masip J, Pang PS, Werdan K, Teichman SL, Trapani A, Bush CA, Saini R, Schumacher C, Severin TM, Metra M. Serelaxin, recombinant human relaxin-2, for treatment of acute heart failure (RELAX-AHF): a randomised, placebo-controlled trial. *Lancet*. 2013;381:29–39.
- Metra M, Ponikowski P, Cotter G, Davison BA, Felker GM, Filippatos G, Greenberg BH, Hua TA, Severin T, Unemori E, Voors AA, Teerlink JR. Effects of serelaxin in subgroups of patients with acute heart failure: results from RELAX-AHF. *Eur Heart J*. 2013;34:3128–3136.

12. Metra M, Cotter G, Davison BA, Felker GM, Filippatos G, Greenberg BH, Ponikowski P, Unemori E, Voors AA, Adams KF Jr, Dorobantu MI, Grinfeld L, Jondeau G, Marmor A, Masip J, Pang PS, Werdan K, Prescott MF, Edwards C, Teichman SL, Trapani A, Bush CA, Saini R, Schumacher C, Severin T, Teerlink JR; RELAX-AHF Investigators. Effect of serelaxin on cardiac, renal, and hepatic biomarkers in the Relaxin in Acute Heart Failure (RELAX-AHF) development program: correlation with outcomes. *J Am Coll Cardiol*. 2013;61:196–206.
13. Samuel CS, Bodaragama H, Chew JY, Widdop RE, Royce SG, Hewitson TD. Serelaxin is a more efficacious antifibrotic than enalapril in an experimental model of heart disease. *Hypertension*. 2014;64:315–322.
14. Samuel CS, Unemori EN, Mookerjee I, Bathgate RAD, Layfield SL, Mak J, Tregear GW, Du X-J. Relaxin modulates cardiac fibroblast proliferation, differentiation, and collagen production and reverses cardiac fibrosis in vivo. *Endocrinology*. 2004;145:4125–4133.
15. Parikh A, Patel D, McTiernan CF, Xiang W, Haney J, Yang L, Lin B, Kaplan AD, Bett GCL, Rasmussen RL, Shroff SG, Schwartzman D, Salama G. Relaxin suppresses atrial fibrillation by reversing fibrosis and myocyte hypertrophy and increasing conduction velocity and sodium current in spontaneously hypertensive rat hearts. *Circ Res*. 2013;113:313–321.
16. Samuel CS. Relaxin: antifibrotic properties and effects in models of disease. *Clin Med Res*. 2005;3:241–249.
17. Hao W, Garcia A, Gao C, Sermadiris I. Relaxin fusion polypeptides and uses thereof. Patent publication No. WO 2018138170. 2018.
18. Murray DR, Mummid S, Valente AJ, Yoshida T, Somanna NK, Delafontaine P, Dinarello CA, Chandrasekar B.  $\beta_2$  Adrenergic activation induces the expression of IL-18 binding protein, a potent inhibitor of isoproterenol induced cardiomyocyte hypertrophy in vitro and myocardial hypertrophy in vivo. *J Mol Cell Cardiol*. 2012;52:206–218.
19. Chen S, Law CS, Grigsby CL, Olsen K, Hong T-T, Zhang Y, Yeghiazarians Y, Gardner DG. Cardiomyocyte-specific deletion of the vitamin D receptor gene results in cardiac hypertrophy. *Circulation*. 2011;124:1838–1847.
20. Zhang G-X, Ohmori K, Nagai Y, Fujisawa Y, Nishiyama A, Abe Y, Kimura S. Role of AT1 receptor in isoproterenol-induced cardiac hypertrophy and oxidative stress in mice. *J Mol Cell Cardiol*. 2007;42:804–811.
21. Menazza S, Sun J, Appachi S, Chambliss KL, Kim SH, Aponte A, Khan S, Katzenellenbogen JA, Katzenellenbogen BS, Shaul PW, Murphy E. Non-nuclear estrogen receptor alpha activation in endothelium reduces cardiac ischemia-reperfusion injury in mice. *J Mol Cell Cardiol*. 2017;107:41–51.
22. Sun J, Aponte AM, Menazza S, Gucek M, Steenbergen C, Murphy E. Additive cardioprotection by pharmacological postconditioning with hydrogen sulfide and nitric oxide donors in mouse heart: S-sulphydration vs. S-nitrosylation. *Cardiovasc Res*. 2016;110:96–106.
23. Sun J, Nguyen T, Aponte AM, Menazza S, Kohr MJ, Roth DM, Patel HH, Murphy E, Steenbergen C. Ischaemic preconditioning preferentially increases protein S-nitrosylation in subsarcolemmal mitochondria. *Cardiovasc Res*. 2015;106:227–236.
24. Chen S, Perlman A, Spanski N, Peterson C, Sanders S, Jaffe R, Martin M, Yalcinkaya T, Cefalo R, Chescheir N. The pharmacokinetics of recombinant human relaxin in nonpregnant women after intravenous, intravaginal, and intracervical administration. *Pharm Res*. 1993;10:834–838.
25. Cossum P, Dwyer K, Roth M, Chen S, Moffat B, Vandlen R, Ferraiolo B. The disposition of a human relaxin (hRlx-2) in pregnant and nonpregnant rats. *Pharm Res*. 1992;9:419–424.
26. Hsu SY, Nakabayashi K, Nishi S, Kumagai J, Kudo M, Sherwood OD, Hsueh AJW. Activation of orphan receptors by the hormone relaxin. *Science*. 2002;295:671–674.
27. Moore X-L, Su Y, Fan Y, Zhang Y-Y, Woodcock EA, Dart AM, Du X-J. Diverse regulation of cardiac expression of relaxin receptor by  $\alpha_1$ - and  $\beta_1$ -adrenoceptors. *Cardiovasc Drugs Ther*. 2014;28:221–228.
28. Leo C, Jelinic M, Ng H, Marshall S, Novak J, Tare M, Conrad K, Parry L. Vascular actions of relaxin: nitric oxide and beyond. *Br J Pharmacol*. 2017;174:1002–1014.
29. Masini E, Bani D, Bello MG, Bigazzi M, Mannaioni PF, Sacchi TB. Relaxin counteracts myocardial damage induced by ischemia-reperfusion in isolated guinea pig hearts: evidence for an involvement of nitric oxide. *Endocrinology*. 1997;138:4713–4720.
30. Valle Raleigh J, Mauro AG, Devarakonda T, Marchetti C, He J, Kim E, Filippone S, Das A, Toldo S, Abbate A, Salloum FN. Reperfusion therapy with recombinant human relaxin-2 (Serelaxin) attenuates myocardial infarct size and NLRP3 inflammasome following ischemia/reperfusion injury via eNOS-dependent mechanism. *Cardiovasc Res*. 2017;113:609–619.
31. Dimmeler S, Fleming I, Fisslthaler B, Hermann C, Busse R, Zeiher AM. Activation of nitric oxide synthase in endothelial cells by Akt-dependent phosphorylation. *Nature*. 1999;399:601–605.
32. Michel JB, Feron O, Sacks D, Michel T. Reciprocal regulation of endothelial nitric-oxide synthase by  $\text{Ca}^{2+}$ -calmodulin and caveolin. *J Biol Chem*. 1997;272:15583–15586.
33. Sun J, Aponte AM, Kohr MJ, Tong G, Steenbergen C, Murphy E. Essential role of nitric oxide in acute ischemic preconditioning: S-nitrosylation versus sGC/cGMP/PKG signaling? *Free Radic Biol Med*. 2013;54:105–112.
34. Sun J, Kohr MJ, Nguyen T, Aponte AM, Connelly PS, Esfahani SG, Gucek M, Daniels MP, Steenbergen C, Murphy E. Disruption of caveolae blocks ischemic preconditioning-mediated S-nitrosylation of mitochondrial proteins. *Antioxid Redox Signal*. 2012;16:45–56.
35. Sun J, Morgan M, Shen R-F, Steenbergen C, Murphy E. Preconditioning results in S-nitrosylation of proteins involved in regulation of mitochondrial energetics and calcium transport. *Circ Res*. 2007;101:1155–1163.
36. Sun J, Picht E, Ginsburg KS, Bers DM, Steenbergen C, Murphy E. Hypercontractile female hearts exhibit increased S-nitrosylation of the L-type  $\text{Ca}^{2+}$  channel  $\alpha_1$  subunit and reduced ischemia/reperfusion injury. *Circ Res*. 2006;98:403–411.
37. Sun J. Protein S-nitrosylation: a role of nitric oxide signaling in cardiac ischemic preconditioning. *Sheng Li Xue Bao*. 2007;59:544–552.
38. Sun J, Murphy E. Protein S-nitrosylation and cardioprotection. *Circ Res*. 2010;106:285–296.
39. Sun J, Steenbergen C, Murphy E. S-nitrosylation: NO-related redox signaling to protect against oxidative stress. *Antioxid Redox Signal*. 2006;8:1693–1705.
40. Du X-J, Samuel CS, Gao X-M, Zhao L, Parry LJ, Tregear GW. Increased myocardial collagen and ventricular diastolic dysfunction in relaxin deficient mice: a gender-specific phenotype. *Cardiovasc Res*. 2003;57:395–404.
41. Leggabe ED, Royce SG, Hewitson TD, Tang MLK, Zhao C, Moore XL, Tregear GW, Bathgate RAD, Du X-J, Samuel CS. The effects of relaxin and estrogen deficiency on collagen deposition and hypertrophy of nonreproductive organs. *Endocrinology*. 2006;147:5575–5583.
42. Samuel C, Zhao C, Bathgate R, Du X, Summers R, Amento E, Walker L, McBurnie M, Zhao L, Tregear G. The relaxin gene-knockout mouse: a model of progressive fibrosis. *Ann N Y Acad Sci*. 2005;1041:173–181.
43. Devarakonda T, Salloum FN. Heart disease and relaxin: new actions for an old hormone. *Trends Endocrinol Metab*. 2018;29:338–348.
44. Bathgate RA, Halls ML, van der Westhuizen ET, Callander GE, Kocan M, Summers RJ. Relaxin family peptides and their receptors. *Physiol Rev*. 2013;93:405–480.
45. Nistri S, Bani D. Relaxin receptors and nitric oxide synthases: search for the missing link. *Reprod Biol Endocrinol*. 2003;1:5.
46. Wang C, Kemp-Harper BK, Kocan M, Ang SY, Hewitson TD, Samuel CS. The anti-fibrotic actions of relaxin are mediated through a NO-sGC-cGMP-dependent pathway in renal myofibroblasts in vitro and enhanced by the NO donor, diethylamine NONOate. *Front Pharmacol*. 2016;7:91.
47. Saura M, Zaragoza C, Herranz B, Grier A, Diez-Marqués L, Rodriguez-Puyol D, Rodriguez-Puyol M. Nitric oxide regulates transforming growth factor-beta signaling in endothelial cells. *Circ Res*. 2005;97:1115–1123.
48. Lima B, Forrester MT, Hess DT, Stamler JS. S-nitrosylation in cardiovascular signaling. *Circ Res*. 2010;106:633–646.
49. Murphy E, Kohr M, Menazza S, Nguyen T, Evangelista A, Sun J, Steenbergen C. Signaling by S-nitrosylation in the heart. *J Mol Cell Cardiol*. 2014;73:18–25.
50. Schulman IH, Hare JM. Regulation of cardiovascular cellular processes by S-nitrosylation. *Biochim Biophys Acta*. 2012;1820:752–762.
51. Beigi F, Gonzalez DR, Minhas KM, Sun Q-A, Foster MW, Khan SA, Treuer AV, Dulce RA, Harrison RW, Saraiva RM, Premer C, Schulman IH, Stamler JS, Hare JM. Dynamic denitrosylation via S-nitrosoglutathione reductase regulates cardiovascular function. *Proc Natl Acad Sci USA*. 2012;109:4314–4319.
52. Malik M, Shukla A, Amin P, Nieldelmann W, Lee J, Jividen K, Phang JM, Ding J, Suh KS, Curmi PMG, Yuspa SH. S-nitrosylation regulates nuclear translocation of chloride intracellular channel protein CLIC4. *J Biol Chem*. 2010;285:23818–23828.
53. Menazza S, Aponte A, Sun J, Gucek M, Steenbergen C, Murphy E. Molecular signature of nitroso-redox balance in idiopathic dilated cardiomyopathies. *J Am Heart Assoc*. 2015;4:e002251. DOI: 10.1161/JAHA.115.002251.
54. Irwin C, Roberts W, Irwin C, Roberts W, Naseem KM. Nitric oxide inhibits platelet adhesion to collagen through cGMP-dependent and independent mechanisms: the potential role for S-nitrosylation. *Platelets*. 2009;20:478–486.
55. Gu Z, Kaul M, Yan B, Kridel SJ, Cui J, Strongin A, Smith JW, Liddington RC, Lipton SA. S-nitrosylation of matrix metalloproteinases: signaling pathway to neuronal cell death. *Science*. 2002;297:1186–1190.
56. Lai T, Hausladen A, Slaughter T, Eu J, Stamler J, Greenberg C. Calcium regulates S-nitrosylation, denitrosylation, and activity of tissue transglutaminase. *Biochemistry*. 2001;40:4904–4910.